THE JOURNAL OF BIOLOGICAL CHEMISTRY VOL. 282, NO. 12, pp. 8777–8785, March 23, 2007

Characterization of Mutants That Change the Hydrogen Bonding of the Semiquinone Radical at the Q_H Site of the Cytochrome bo_3 from *Escherichia coli*[*] [S]

Received for publication, December 19, 2006, and in revised form, January 22, 2007 Published, JBC Papers in Press, January 30, 2007, DOI 10.1074/jbc.M611595200

Lai Lai Yap[‡], Rimma I. Samoilova[§], Robert B. Gennis[‡1], and Sergei A. Dikanov[¶2]

From the Departments of [‡]Biochemistry and [¶]Veterinary Clinical Medicine, University of Illinois, Urbana, Illinois 61801 and the [§]Institute of Chemical Kinetics and Combustion, Russian Academy of Sciences, Novosibirsk 630090, Russia

The cytochrome bo_3 ubiquinol oxidase catalyzes the two-electron oxidation of ubiquinol in the cytoplasmic membrane of *Escherichia coli*, and reduces O_2 to water. This enzyme has a high affinity quinone binding site (Q_H), and the quinone bound to this site acts as a cofactor, necessary for rapid electron transfer from substrate ubiquinol, which binds at a separate site (Q_L), to heme *b*. Previous pulsed EPR studies have shown that a semiquinone at the Q_H site formed during the catalytic cycle is a neutral species, with two strong hydrogen bonds to Asp-75 and either Arg-71 or Gln-101. In the current work, pulsed EPR studies have been extended to two mutants at the Q_H site. The D75E mutation has little influence on the catalytic activity, and the pattern of hydrogen bonding is similar to the wild type. In contrast, the D75H mutant is virtually inactive. Pulsed EPR revealed significant structural changes in this mutant. The hydrogen bond to Arg-71 or Gln-101 that is present in both the wild type and D75E mutant oxidases is missing in the D75H mutant. Instead, the D75H has a single, strong hydrogen bond to a histidine, likely His-75. The D75H mutant stabilizes an anionic form of the semiquinone as a result of the altered hydrogen bond network. Either the redistribution of charge density in the semiquinone species, or the altered hydrogen bonding network is responsible for the loss of catalytic function.

Escherichia coli cytochrome (cyt)[3] bo_3 ubiquinol oxidase catalyzes the two-electron oxidation of ubiquinol and the four-electron reduction of O_2 to water. The enzyme contains three redox-active metal centers: a low spin heme *b*, which is involved in quinol oxidation, and the heme o_3/Cu_B bimetallic center, which is the site where O_2 binds and is reduced to water. The ubiquinol oxidation occurs with a semiquinone (SQ) intermediate in an overall reaction that releases two protons to the periplasm. The enzyme contains two Q sites (1–6): a low affinity site (Q_L), which is equilibrated with the quinone pool in the membrane and functions as the substrate (QH_2) binding site, and a high affinity (Q_H) site, from which Q is not readily removed, and that stabilizes a SQ (7–10). The quinone bound at the high-affinity site appears to function as a tightly bound cofactor, similar to the Q_A site of the reaction centers. Rapid kinetic studies show that the quinone bound at the Q_H site is important for rapid reduction of heme *b* but not for rapid electron transfer from heme *b* to the heme o_3/Cu_B binuclear center (11, 12). The heme o_3/Cu_B site is where O_2 is reduced to H_2O using the electrons provided by the oxidation of quinol. Hence, the suggested electron transfer sequence is as follows in Reaction 1.

$$Q_LH_2 \rightarrow Q_H \rightarrow \text{heme } b \rightarrow \text{heme } o_3/Cu_B \rightarrow O_2$$

REACTION 1

The x-ray structure of cytochrome bo_3 (13) does not contain any bound quinone, but site-directed mutagenesis studies (2–4, 13) have identified residues that modulate the properties of the Q_H site. The model of the Q_H quinone binding site (Fig. 1), including Arg-71, Asp-75, His-98, and Gln-101 residues (13), has been explored by site-directed mutagenesis (2, 13). The R71H, H98F, D75H, and I102W mutant enzymes were found to show very little or no quinol oxidase activity. No EPR signal was observed for the H98F and R71H mutants. A SQ signal was detected in the same potential range as that of the wild type enzyme for the D75H mutant. However, the EPR spectrum of the D75H mutant lacks the characteristic hyperfine structure, indicating a significant change in the hydrogen bonding of the SQ. For the I102W mutant, a radical signal was seen with a redox midpoint potential downshifted by about 200 mV. On the basis of these observations it was suggested that Arg-71, Asp-75, and His-98 are involved in the stabilization of the SQ in the Q_H site.

The interaction of the SQ with the protein environment in cytochrome bo_3 has been characterized by pulsed EPR spectroscopy. ESEEM data show that there is one H-bond to the Q_H SQ from a nitrogen atom of the side chain of an arginine or glutamine (5, 6, 14). Candidates are the side chain of either Arg-71 or Gln-101 (14). An H-bond to His-98 is definitively ruled out.

Further information was obtained from two-dimensional ESEEM (14) in conjunction with ^1H_2O and ^2H_2O exchange, indicating at least three exchangeable protons. Two of the pro-

* This work was supported by National Institutes of Health Grant GM62954 (to S. A. D.), Department of Energy Grant DE-FG02-87ER13716 (to R. B. G.), Fogarty Grant PHS 1 RO3 TW 01495 (to R. I. S.), and NCRR, National Institute of Health Grant S10-RR15878 for instrumentation. The costs of publication of this article were defrayed in part by the payment of page charges. This article must therefore be hereby marked "*advertisement*" in accordance with 18 U.S.C. Section 1734 solely to indicate this fact.

[S] The on-line version of this article (available at http://www.jbc.org) contains supplemental Figs. S1–S7 and Tables S1–S2.

[1] To whom correspondence may be addressed. E-mail: r-gennis@uiuc.edu.
[2] To whom correspondence may be addressed. E-mail: dikanov@uiuc.edu.

[3] The abbreviations used are: cytochrome bo_3, cytochrome bo_3 ubiquinol oxidase from *E. coli*; SQ, semiquinone; Q_H, the high affinity quinone-binding site; EPR, electron paramagnetic resonance; ESEEM, electron spin echo envelope modulation; HYSCORE, hyperfine sublevel correlation; ENDOR, electron-nuclear double resonance.

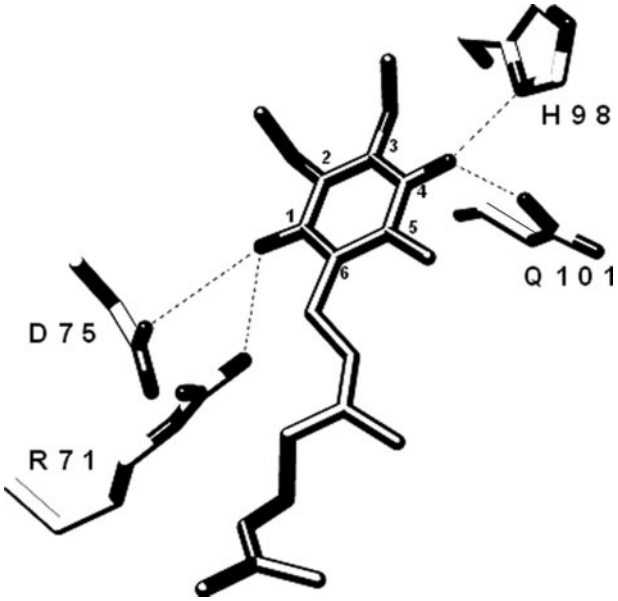

FIGURE 1. **Model of the quinone binding at the Q_H site of the *cytochrome* bo_3.** The figure was generated according to the model based on the x-ray crystal structure by Abramson *et al.* (13).

tons possess large anisotropic hyperfine couplings (~4 and 6 MHz), and were assigned to the protons interacting with carbonyl oxygens. The ENDOR and two-dimensional ESEEM spectra were also used to determine that the isotropic hyperfine constant with the non-exchangeable methyl protons of the SQ in cytochrome bo_3 is ~10–11 MHz (14–16). This value is about twice the coupling for UQ anion radicals in solution. This large hyperfine coupling, along with the value of the anisotropic hyperfine coupling of ~6 MHz for one exchangeable proton, are consistent with the SQ being a *neutral radical*, protonated at carbonyl oxygen O-1, rather than an anion radical (14). The exchangeable proton with 4 MHz coupling could be a proton shared either between quinone carbonyl O-1 and a nitrogen-containing group of Arg-71 or between carbonyl O-4 and the NH_2 group of Gln-101 (see Fig. 1).

The current work is motivated by the previous observation that the D75H mutant is virtually inactive, but the midpoint potential and stability of the SQ bound at the Q_H site are virtually unchanged (2). The loss of activity due to the D75H mutation correlates with a change in the line shape of the EPR spectrum of the SQ. The change in line shape implies an altered environment around the SQ. The specific nature of the changes of the SQ environment is explored in the current work by the application of high resolution EPR spectroscopy. The major finding is that the D75H mutation results in stabilizing the anionic form of the SQ at the Q_H site, which correlates with the loss of enzyme activity.

EXPERIMENTAL PROCEDURES

Sample Preparation—The *cyoABCDE* operon encoding cytochrome bo_3 with a His_6 tag at the C terminus end of subunit II was cloned into the pET-17b vector (Novagen). The D75H and D75E mutants were constructed using the QuikChange site-directed mutagenesis kit from Stratagene, and the primers were synthesized by Bio-Synthesis (Bio-Synthesis, Inc.). The mutations were verified by partial sequencing of the gene. The mutant proteins were expressed in the C43(DE3) *E. coli* strain (Avidis, France) in which *cyoBCD* was deleted. Overexpression of the mutant proteins was achieved by induction with isopropyl 1-thio-β-D-galactopyranoside at 37 °C. Harvested cells were resuspended in 50 mM K_2HPO_4, 5 mM $MgSO_4$, pH 8.3, and broken by passing through a microfluidizer (Microfluidics Corp.) at 10,000 p.s.i. for a total of 3 times. The lysate was centrifuged at 16,000 × *g* for 30 min to remove cell debris. Membranes were then isolated from the supernatant by centrifugation at 180,000 × *g* for 5 h. The isolated membranes were suspended in 50 mM K_2HPO_4, pH 8.3, and solubilized with 1% *n*-dodecyl β-D-maltoside (Anatrace) by stirring at 4 °C for 2 h, followed by centrifugation at 15,000 × *g* for 1 h to remove unsolubilized material. The solubilized enzyme was loaded onto a nickel-nitrilotriacetic acid column and purified as described previously (17). The purified protein was dialyzed in 50 mM K_2HPO_4, 0.1% *n*-dodecyl β-D-maltoside, pH 8.3, and concentrated to ~600 μM. For the deuterated sample, the dialyzed protein was concentrated, exchanged with deuterated 50 mM K_2HPO_4, 0.1% *n*-dodecyl β-D-maltoside, pD 8.3, and then further concentrated to ~600 μM. The enzyme was anaerobically reduced under an argon atmosphere with 500 times excess sodium ascorbate. The reduced sample was quickly transferred to an argon-flushed EPR tube and rapidly frozen in liquid nitrogen.

EPR Measurements—The CW EPR measurements were performed on an X-band Varian EPR-E122 spectrometer at 100 K. The pulsed EPR experiments were carried out using an X-band Bruker ELEXSYS E580 spectrometer equipped with Oxford CF 935 cryostats. Unless otherwise indicated, all measurements were made at 50 K. Some pulsed EPR measurements were also performed at higher temperatures, up to 120 K, and the results were similar to those obtained at 50 K. Several types of ESE experiments with different pulse sequences were employed with appropriate phase cycling schemes to eliminate unwanted features from the experimental echo envelopes. Among them are one-dimensional and two-dimensional three-pulse and four-pulse sequences, which are described in detail elsewhere (14). Spectral processing of three- and four-pulse ESEEM patterns, including subtraction of relaxation decay (fitting by 3–4 degree polynomials), apodization (Hamming window), zero feeling, and fast Fourier transformation, was performed using Bruker WIN-EPR software.

Pulsed ENDOR spectra of the radicals were obtained using Davies and Mims sequences with different pulse lengths. The specifics of these experiments are described in detail elsewhere (19).

Characteristics of HYSCORE Spectra from $I = ½$ Nuclei—The most informative experimental data regarding the ligand environment of the semiquinone were obtained from the two-dimensional ESEEM (HYSCORE) experiment (18). The basic advantage of the HYSCORE technique is the creation of two-dimensional spectra with off-diagonal cross-peaks (ν_α, ν_β) and (ν_β, ν_α), whose coordinates are nuclear frequencies from opposite electron spin manifolds. Orientationally disordered (*i.e.* powder) two-dimensional spectra of $I = ½$ nuclei also reveal, in the form of cross-peak contour projections, the interdepen-

dence between ν_α and ν_β values in the same orientation. Analysis of the contours allows for direct, simultaneous determination of the nuclear isotropic and anisotropic hyperfine coupling constants (20).

The "Cancellation Condition" in ^{14}N ESEEM Spectra—Because of the $I = 1$ spin, and the quadrupole interactions resulting from this, the ^{14}N nucleus can produce up to six lines in an ESEEM spectrum, three from each of the two electron spin manifolds with $m_S = +½$ or $-½$. In measurements of amorphous (powder) samples, such as the frozen suspensions of cytochrome bo_3 used in this work, because of their different orientation dependence, not all transitions contribute equally to the spectra. The type of spectrum expected from ^{14}N with predominantly isotropic hyperfine coupling A is governed by the ratio between the effective nuclear frequency in each manifold, $\nu_{ef\pm}$, given by $\nu_{ef\pm} = |\nu_N \pm |A|/2|$ (ν_N is the Zeeman frequency of ^{14}N), and the quadrupole coupling constant, K, given by $K = e^2qQ/4h$ (21, 22).

If $\nu_{ef\pm}/K \sim 0$, *i.e.* $\nu_{ef\pm} \cong 0$ (the situation called a cancellation condition because $\nu_N \cong A/2$) then the three nuclear frequencies from a corresponding manifold will be close to the three pure (or zero field) nuclear quadrupole resonance frequencies of ^{14}N. In this case, three narrow peaks at the frequencies ν_+, ν_-, and ν_o will appear in the powder ESEEM spectra, with the property $\nu_+ = \nu_- + \nu_0$.

$$\nu_+ = K(3 + \eta); \quad \nu_- = K(3 - \eta); \quad \nu_0 = 2K\eta \qquad \text{(Eq. 1)}$$

The frequencies, described by Equation 1 can appear in spectra up to a ratio of $\nu_{ef\pm}/K \sim 0.75$–1, but are broadened as this value departs from 0 (21, 22). The term η is an asymmetry parameter.

If $\nu_{ef\pm}/K > 1$, only a single line is expected from each corresponding manifold without any pronounced orientation dependence. This line is produced by a transition at the maximum frequency, which is actually a double-quantum transition between the two outer states with $m_I = -1$ and $+1$. The frequency of this transition is well described by Equation 2,

$$\nu_{dq\pm} = 2[\nu^2_{ef\pm} + \kappa]^{1/2} \qquad \text{(Eq. 2)}$$

where $\kappa = K^2(3 + \eta^2)$ (21). Two other single-quantum transitions, involving the central level with $m_I = 0$, have a significant orientation dependence from quadrupole interaction and could produce lines at varying frequencies in the orientation-selected spectra.

Thus, the three-pulse ESEEM spectrum near the cancellation condition will consist of four lines, *i.e.* three narrow lines at zero-field nuclear quadrupole resonance frequencies, described by Equation 1, from manifold with $\nu_{ef} \sim 0$, and one double-quantum transition from the opposite manifold described by Equation 2.

RESULTS

EPR Spectra—Fig. 2 shows the X-band EPR spectra of the semiquinone in the wild type cytochrome bo_3, along with the D75E and D75H mutants. The SQ spectra all display a single line with similar g value about 2.0047 ± 0.0001. The difference between the spectra is in the weakly resolved hyperfine structure due to coupling with the methyl protons (6, 15). The hyperfine structure, which is readily seen in the spectrum of wild type protein, is also present in the spectrum of D75E mutant oxidase, but it is absent in the spectrum from D75H.

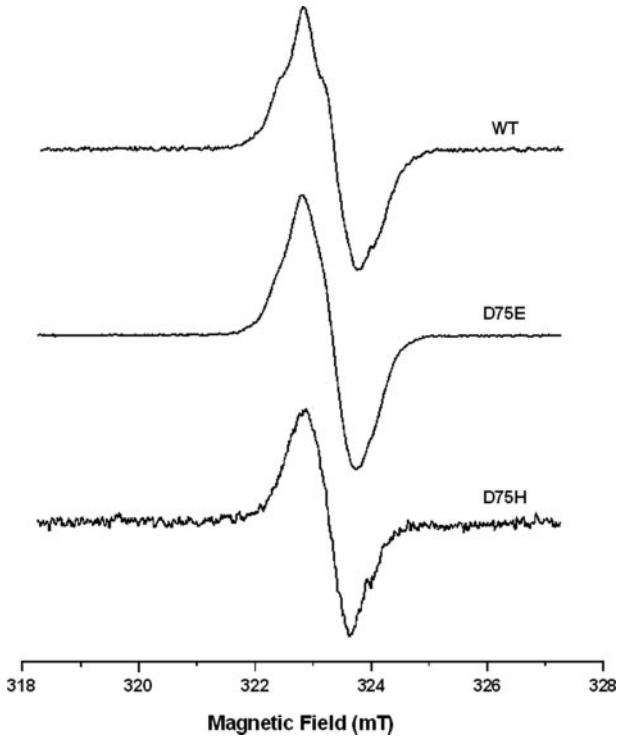

FIGURE 2. **X-band EPR spectra of the semiquinone radical in wild type (*WT*), D75E mutant and D75H mutant cytochrome bo_3 from *E. coli*.** EPR conditions: sample temperature, 100 K; modulation frequency, 100 kHz; modulation amplitude, 0.2 millitesla; microwave power, 0.2 milliwatt; microwave frequency, 9.08 GHz. The concentrations of the wild type, D75E, and D75H mutants were all 100 μM. However, the signal-to-noise ratio for the D75H mutant is smaller because this mutant can only generate ~20–25% of the semiquinone radical compared with the wild type and D75E mutant.

Nitrogens Detected by ESEEM in Wild Type Protein and Mutants—Fig. 3 shows the stacked plots of the three-pulse ESEEM spectra at frequencies <10 MHz, appropriate for ^{14}N nuclei, recorded as a function of time, τ, between the first and second pulses at the maximum of the EPR intensity for the SQ in the wild type, D75E, and D75H oxidases. Each spectrum exhibits three-intensive narrow lines ν_0, ν_-, and ν_+ with a property $\nu_0 + \nu_- = \nu_+$. There is also a less intensive and broader line at frequency ν_{dq} (21, 22). These spectra have a shape typical for a single ^{14}N recorded near cancellation conditions, and allows for an immediate assignment of the narrow peaks to three nuclear quadrupole resonance frequencies (see Equation 1), and for the frequency of the double-quantum transition ν_{dq} (see Equation 2). This assignment was confirmed by the ^{14}N HYSCORE spectra. These spectra (Fig. S1 in supplementary materials) exhibit cross-peaks correlating ν_0, ν_-, and ν_+ with ν_{dq}, thus indicating that they belong to different manifolds. They also allow determining more precisely the value of the ν_{dq} frequency from the (ν_{dq},ν_+) cross-correlation possessing maximum intensity.

Having obtained the frequencies for ν_0, ν_-, ν_+, and ν_{dq}, Equations 1 and 2 along with the ^{14}N Zeeman frequency (ν_N = 1.065 MHz) were used to determine the quadrupole coupling

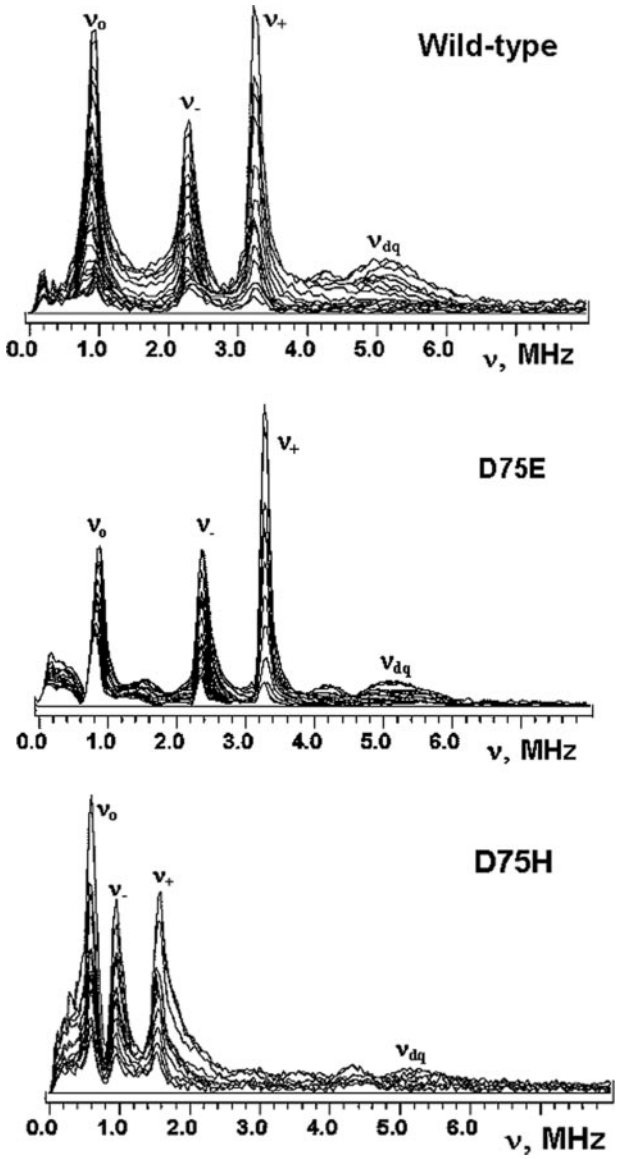

FIGURE 3. **Stacked plots of three-pulse ESEEM spectra of the SQ at the Q_H site of wild type cytochrome bo_3, D75E, and D75H mutants.** The spectra show modulus Fourier transforms along the time T (between second and third microwave pulses) axis (512 points with a 16 ns step) at different times τ. The initial time τ (between first and second pulses) is 88 ns in the farthest trace and was increased by 16 ns in successive traces. The microwave frequency was 9.7 GHz, and the magnetic field was 346.0 millitesla.

constant K, the asymmetry parameter η, and the hyperfine coupling A with the nitrogen nuclei. Their values for three proteins are collected in Table 1. Thus, the SQ in the wild type, D75H, and D75E mutant oxidases each interacts only with a single nitrogen carrying significant, presumably isotropic hyperfine coupling resulting from the transfer of the unpaired spin density from the SQ via the hydrogen bond bridge. The values of K and η characterize the chemical type of ^{14}N nucleus interacting with the SQ.

The characteristics of the nitrogen in the D75E mutant is only slightly changed compared with that observed in the wild type oxidase, indicating that the same nitrogen, previously assigned to either the Arg-71 or Gln-101 side chain in the wild type enzyme (14), is also hydrogen bonded to the SQ in the

TABLE 1
^{14}N ESEEM frequencies in wild type cytochrome bo_3, D75E, and D75H mutants, and nuclear quadrupole and hyperfine parameters

Protein	ν_0	ν_-	ν_+	ν_{dq}	K	η	A
		MHz[a]		*MHz*			*MHz*
Wild type	0.95	2.32	3.27	5.1–5.2	0.93	0.51	1.8
D75E	0.90	2.41	3.31	5.1–5.2	0.95	0.47	1.9
D75H	0.63	0.98	1.61	5.0–5.1	0.43	0.73	2.7

[a] An accuracy in the determination of the nqr frequencies ±0.03 MHz.

D75E mutant. In contrast, the quadrupole coupling constant of the nitrogen in the D75H mutant is more than two times smaller than that of the nitrogen in the wild type oxidase, showing that the nitrogen H-bonded to the SQ in the D75H mutant is from a different chemical group. Hence, the hydrogen bond of the SQ to Arg-71 or Gln-101 that is present in the wild type enzyme is broken (or significantly weakened) in the D75H mutant, and is replaced by a strong hydrogen bond to different nitrogen. Additional information about the H-bonds in these proteins was obtained from the study of the proton environment of the SQ.

Proton HYSCORE and ESEEM—Fig. 4 shows the proton part of the HYSCORE spectra (τ = 136 ns) of the SQ radical in the D75E and D75H samples prepared in ^1H_2O and ^2H_2O buffer. The spectrum of wild type cytochrome bo_3 has been discussed previously (14) and is shown for convenience in supplementary materials Fig. S2. In addition to a diagonal peak with extended shoulders at the proton Zeeman frequency ($\nu_H \sim 14.7$ MHz), the spectra of the D75E and D75H samples in ^1H_2O (Fig. 4) contain several pairs of resolved cross-peaks located symmetrically relative to the diagonal. Among those, only cross-peaks with maximal splitting (**1**) and the diagonal peak, with its shoulders, still appear in the spectra obtained under the same conditions using the samples with ^2H_2O. All other cross-peaks **2**–**4** completely disappear in these spectra, showing that these are produced by exchangeable protons.

One obvious difference between the spectra from the D75E and D75H mutants is that in the D75E spectrum, the nonexchangeable cross-peaks (**1**) produced by the methyl protons (14) are well separated from the cross-peaks of the exchangeable protons, whereas in the D75H spectrum, these cross-peaks are overlapped due to smaller coupling with methyl protons. The wild type spectrum is similar to that from D75E in this respect.

Quantitative analysis of the cross-peak contour line shapes and simulations of the spectra, described in detail in Ref. 14 and under supplementary materials show that cross-peaks **2** and **3** in the spectra of D75E and D75H are produced by the same proton(s). Cross-peaks **4** belong to different proton(s). The analysis provides also the isotropic (a) and anisotropic (T) components of the axial hyperfine tensors, which are summarized in Table 2 for nonexchangeable methyl protons and in Table 3 for exchangeable protons.

Additional information about the exchangeable protons was obtained from the sum combination peaks in the one-dimensional four-pulse ESEEM spectra, which are particularly useful for the observation of proton sum combination lines with improved resolution (23). The four-pulse ESEEM spectrum of the SQ in wild type cytochrome bo_3 in ^1H_2O buffer contains

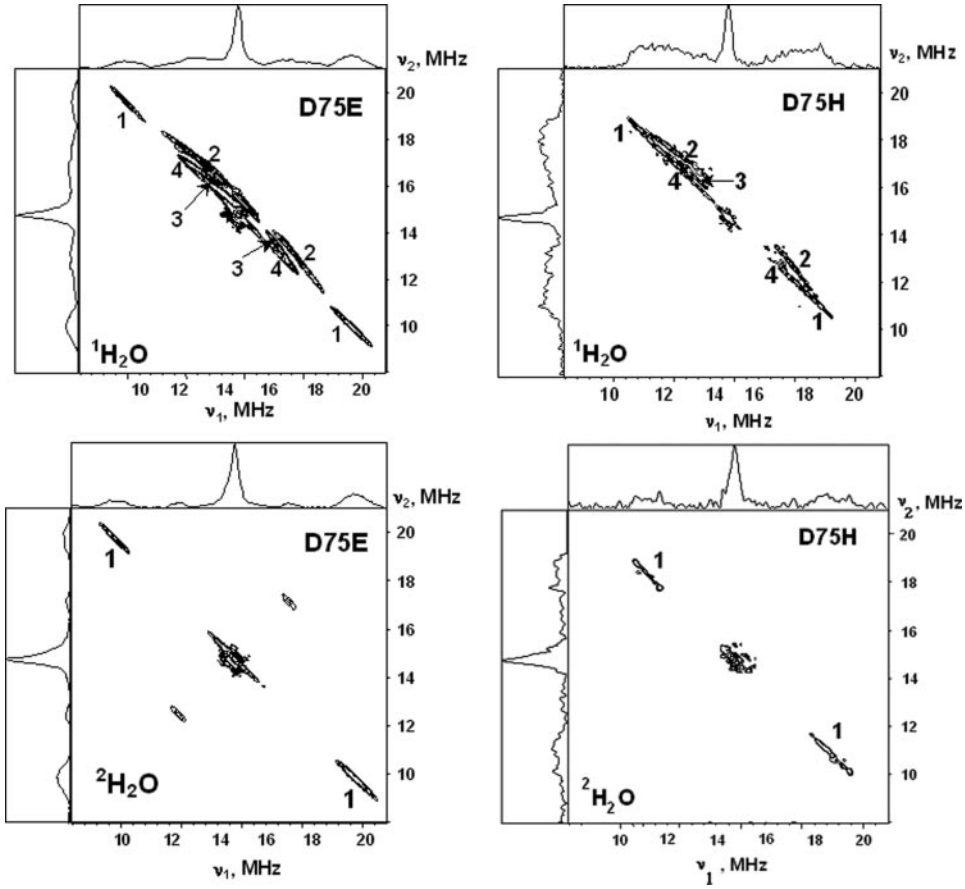

FIGURE 4. **The ^1H HYSCORE spectra of the SQ at the Q_H site of D75E and D75H mutants in ^1H_2O and ^2H_2O.** The microwave frequency was 9.7 GHz, and the magnetic field was 346.0 millitesla, the time τ, between first and second microwave pulses, was 136 ns. Spectra were obtained after Fourier transformation of the two-dimensional time domain patterns containing 256 × 256 points with a 20-ns step.

TABLE 2
Hyperfine tensors of the methyl protons (MHz) derived from HYSCORE spectra

Protein	a	T	$A_\perp = a - T$	$A_\parallel = a + 2T$
Wild-type[a]	10.0	1.7	8.3	13.4
D75E	9.2	1.4	7.8	12.0
D75H	8.0	0.8	7.2	9.6

[a] From Ref. 14.

TABLE 3
Hyperfine tensors of the exchangeable protons
H2-H4 (MHz) derived from HYSCORE spectra.

Proton	a,T		
	Wild-type[a]	D75E	D75H
		MHz	
H2	±0.7, ∓6.3	±0.5, ∓4.7	±1.0, ∓4.6
H3	∓1.2, ±4.2	Close to H2	
H4	∓4.6, ±1.7	∓5.0, ±1.8	∓4.3, ±1.2

[a] From Ref. 14.

three well resolved lines in the region of the proton $2\nu_H$ as shown in Fig. 5. The most intense line appears exactly at the $2\nu_H$ frequency and represents the contribution of weakly coupled protons from the protein environment. The four-pulse spectrum also reveals two peaks of lower intensity (H2 and H3) shifted from $2\nu_H$ to higher frequencies by ~0.7 and ~1.4 MHz. These two shifted lines completely disappear in the spectra of the sample prepared in ^2H_2O. From this, one can conclude that the shifted lines also contain a major contribution from exchangeable protons.

The shifts observed in the four-pulse ESEEM are well described by Equation 3,

$$\Delta = 9T^2/16\nu_H \qquad \text{(Eq. 3)}$$

from which the anisotropic component T can be estimated (23). The shifts of ~0.7 and ~1.4 MHz correspond to T = 4.2 and 6.0 MHz (Table 4), which are consistent with the T values determined for two exchangeable protons with largest hyperfine couplings from HYSCORE spectra (14). All other protons from the SQ and its environment possess smaller hyperfine couplings, which do not give resolvable shifts.

In contrast to the wild type protein, the four-pulse ESEEM spectrum of the D75E mutant shows a single shifted peak of asymmetrical form with a shoulder at the high frequency side. The maximum of this line is shifted 0.75 MHz from the line at $2\nu_H$ that corresponds to the $T \sim 4.5$ MHz matching the value determined from the analysis of the cross-peak contours **2** and **3** in the HYSCORE spectra. However, the asymmetric form of the shifted peak suggests that it represents the overlap of the lines from two protons with close values of the anisotropic coupling. The maximum value of the shift for the second proton can be estimated to be 0.9–1.0 MHz, corresponding to a difference in the anisotropic hyperfine coupling up to ~0.5 MHz (Table 3). Cross-peaks **2** in the HYSCORE spectra of D75E possess the accompanying shoulders (see the enhanced central part of the spectrum in supplemental materials Fig. S5), suggesting that cross-peaks **2** and **3** actually are a superposition of two protons with close couplings and that the hyperfine parameters determined by plotting the coordinates of the ridges with maximum intensity provide average values.

The four-pulse spectrum of the D75H mutant shows one symmetrical peak with the shift 0.8 MHz corresponding to the anisotropic coupling $T \sim 4.6$ MHz similar as determined for the proton H2 from the HYSCORE spectra. The exchangeable protons with weaker couplings ($T \sim 1.2$–1.8 MHz) observed in the HYSCORE spectra of D75E and D75H (Table 3) would produce unresolved shifts of ~0.1 MHz in the four-pulsed spectra.

DISCUSSION

The Nature of H-bonded Nitrogens

Based on the crystal structure of cytochrome bo_3, it was proposed (13) that the carbonyl oxygens of the bound ubiquinol

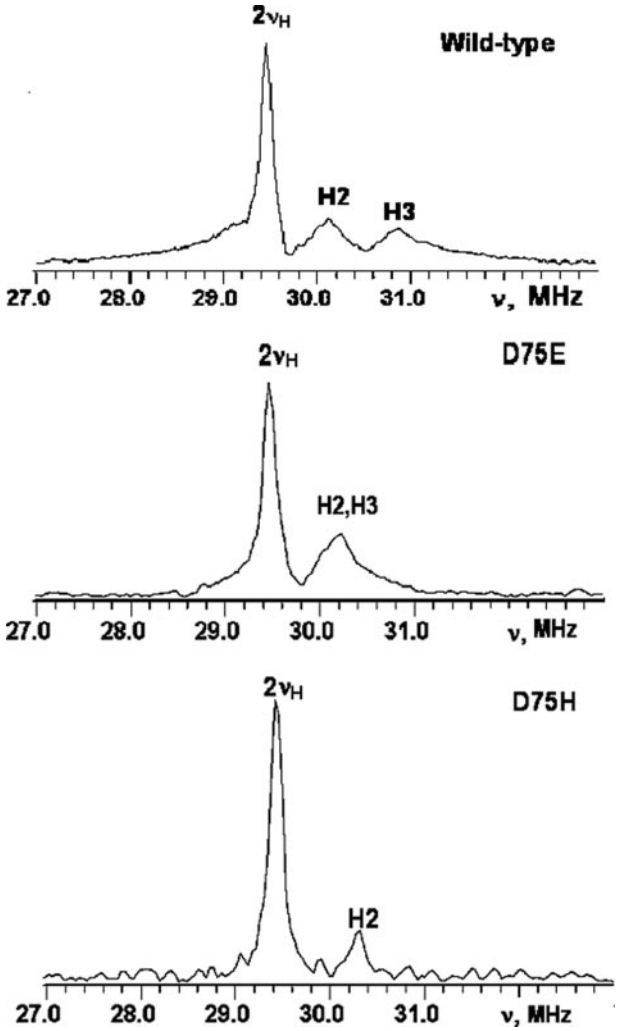

FIGURE 5. **The four-pulse ESEEM spectra of the SQ at the Q_H site of wild type cytochrome bo_3, and the D75E and D75H mutants prepared in H_2O.** The spectra show modulus Fourier transforms along the time *T*/2 axis (800 points with a 12-ns step) at $\tau = 100$ ns.

TABLE 4

The shifts of the sum-combination line from exchangeable protons and the corresponding anisotropic couplings

Protein	Proton	Shift	*T*
		MHz	
Wild-type	H2	1.4	6.0
	H3	0.7	4.2
D75E	H2	0.75	4.5
	H3	Up to 0.9–1.0	~5.0
D75H	H2	0.8	4.6

can form up to four hydrogen bonds to Asp-75, Arg-71, His-98, and Gln-101 in the Q_H site of the wild type protein (Fig. 1). Site-directed mutagenesis studies (2, 13) have confirmed that these four residues are functionally important and that mutants at each position alter or eliminate the SQ that is stabilized at the Q_H site (2). ^{14}N ESEEM data have clearly shown that there is one H-bond to the Q_H SQ from a protein nitrogen atom (5, 6, 14). The value of the quadrupole coupling constant $K = 0.93$ MHz allows one to assign this nitrogen to the NH_2 or NH group of Arg-71 or Gln-101 side chain (14). The measured constant *K* slightly exceeds the quadrupole coupling constant for a peptide nitrogen −NH-C = O, whose values vary between 0.75 and 0.85

TABLE 5

Comparison of nuclear quadrupole tensors and hyperfine couplings for ^{14}N histidine nitrogen involved in hydrogen bond formation with the semiquinone in different quinone processing sites

Semiquinone site	$\|K\|^a$	η	A^a	Ref.
Q_H cytochrome bo_3	0.43	0.73	2.7	This work
Q_A PS II	0.35	0.69	1.7	39
Q_A PS II	0.39	0.69	1.9	40
Q_A in *Rhodobacter sphaeroides*	0.41	0.73		41
Q_A in *Rhodobacter viridis*	0.41	0.69		41
Q_A in *Rb. sphaeroides*	0.38	0.82	1.1 or 1.8	42
Q_B in *Rb. sphaeroides*	0.41	0.61		41

[a] In MHz.

MHz in different compounds and proteins (14). The coupling constant is also larger than the *K* values reported for either the deprotonated or protonated nitrogens of the imidazole residue (see below). That rules out histidine as a hydrogn bond partner to the semiquinone in the wild type oxidase.

The spectra of the D75E mutant indicate that the same residue (Arg-71 or Gln-101) is hydrogen bonded to the SQ in this protein as in the wild type. The substitution of Glu for Asp does result in some relatively minor changes of this H-bond reflected in the values of the proton and nitrogen couplings. Notably, this mutant is catalytically functional.

Substituting histidine for the aspartate at position 75, however, produces substantial changes in the hydrogen bonding of the SQ at the Q_H site. One nitrogen with a considerably smaller quadruple coupling constant ($K = 0.43$ MHz) contributes to the ^{14}N ESEEM spectra of the D75H mutant. The data suggest that the SQ is hydrogen bonded to a protonated imidazole nitrogen of a histidine residue.

The quadrupole parameters reported for the imine (N-δ) and amine (N-ϵ) nitrogens in non-coordinated imidazole and histidine are equal to $K = 0.81–0.84$ MHz ($\eta = 0.13$), and $K = 0.35$ MHz ($\eta = 0.915–0.995$), respectively (24–26). However, when both imidazole nitrogens are protonated, as in *L*-histidine monochloride monohydrate, then the quadrupole parameters become $K = 0.32$ MHz ($\eta = 0.946–0.974$) for N-δ, and $K = 0.366$ MHz ($\eta = 0.268–0.3$) for N-ϵ (26, 27). Only slight variations of the quadrupole coupling constant ($K = 0.35–0.43$ MHz) are observed for the amine imidazole nitrogen in compounds coordinated to Zn^{2+}, Cd^{2+}, or Cu^{2+} or in copper proteins (28–30).

There are examples of hydrogen bonding between a SQ and a histidine nitrogen, specifically N-δ, in other quinone processing sites, based on ESEEM spectroscopy and supported by evidence from x-ray crystallography and Fourier transform infrared spectroscopy. The spectroscopic parameters for these nitrogens are listed in Table 5. They possess $K \sim 0.35–0.41$ MHz and $\eta \sim 0.6–0.8$, which characterize the geometry and population of the electronic orbitals of the nitrogen atom.

The quadrupole characteristics of the nitrogen in D75H are consistent with those previously reported for the protonated imidazole nitrogens in different systems. The spread in the *K* and η values reflect differences in the nitrogen environment, including strength and geometry of the hydrogen bond, resulting in the redistribution of the electron population between the N-H and p_π orbitals (27, 28, 30). Detailed computational analysis of the particular values would require precise knowledge of the nitrogen location relative to the SQ molecule, the N . . .

H . . . O distances and angle. It is clear, however, that in the D75H mutant the strong hydrogen bond to Arg-71 or Gln-101 that is present in the wild type oxidase has been replaced by a hydrogen bond to a histidine. Whether this histidine is the one in place of Asp-75 or is another histidine (*e.g.* His-98) is not known from the spectra.

The Methyl Proton Coupling in Wild Type, D75E, and D75H Mutant Oxidases

In the previously published two-dimensional ESEEM study of the SQ in wild type cytochrome bo_3 it was proposed that the stabilized SQ at the Q_H site is a neutral (*i.e.* protonated) radical (14). All previous ENDOR and ESEEM studies of cytochrome bo_3 (14–16) have found $a = 10–11$ MHz for the methyl protons, which is the largest isotropic hyperfine constant reported for the methyl protons for ubisemiquinones bound to proteins or in solution. Hyperfine coupling of 5.5–6.5 MHz has been reported for ubiquinone anion radicals in different solvents (31–33). The proton isotropic constant of the rotating methyl group is directly proportional to the π-spin density on the attached carbon atom, as described by the McConnel relation $a = 81\rho_\pi$ (34). Thus, the unpaired π-spin density on the carbon attached to the methyl group of the SQ in cytochrome bo_3 is about 2-fold larger (~7 to ~13%) compared with that which is observed with anionic SQ radicals in solution.

Table 2 shows the isotropic and anisotropic components of the hyperfine tensor of the methyl protons in the wild type oxidase, taken from Ref. 14, and in the D75E and D75H mutants (this work). Also shown are the $A_\perp$ and $A_\parallel$ couplings, providing the limiting values for the nuclear frequencies, which vary between $\nu_H \pm A_\parallel/2$ and $\nu_H \pm A_\perp/2$. The ENDOR spectra (supplementary materials Fig. 6S) of the D75H mutant independently confirm the decreased splitting of the methyl protons and their location within the frequency limits shown in Table 2**,** in comparison with wild type protein. There is a progressive decrease of the isotropic hyperfine coupling of the methyl protons from the wild type oxidase, with the largest value, to the D75E mutant, and finally to the D75H mutant. However, even in the case of the D75H mutant, the isotropic hyperfine coupling is still 1.5 times the values of the isotoropic coupling of anion radicals in solution, in which there is symmetrical hydrogen bonding geometry of the O-1 and O-4 carbonyls.

Hydrogen Bonded Protons

Three exchangeable protons with significant differences in their hyperfine couplings were found for the SQ in wild type cytochrome bo_3 (14). Two of these protons possess large anisotropic hyperfine couplings with $|T| = 4.2$ and 6.3 MHz, which exceed the value $|T| \sim 3$ MHz observed for in-plane hydrogen-bonded protons in alcoholic solutions (31, 35, 36). DFT calculations (37) have shown that the hydrogen bonded proton with $|T| \sim 3$ MHz corresponds to an O . . . H distance ~1.8 Å, whereas $|T| = 5.2$ MHz is consistent with a bond distance of 1.4 Å. Hence, the coupling of $|T| = 6.3$ MHz requires an even shorter O . . . H bond distance, of the order 1.2 Å, implying substantial covalent character. This result, together with the value of the proton methyl coupling, provide support for the interpretation that the SQ in wild type cytochrome bo_3 can be considered not as a hydrogen bonded anion but as a protonated neutral radical (14).

The two-dimensional ESEEM study of the mutants shows that the anisotropic hyperfine couplings with the exchangeable protons are changed. The spectra in the D75E mutant show that there are still two strongly coupled exchangeable protons with values of $T \sim 4.7–5$ MHz, corresponding to O . . . H distances of ~1.5 Å (37). Hence, it appears that the hydrogen bond strengths are changed in the D75E mutant, but the hydrogen bond pattern is similar to that of the wild type oxidase.

The D75H mutant, however, is significantly different. There is only one proton with the similar strength of hyperfine coupling and distance shown by the one-dimensional and two-dimensional ESEEM spectra. Any other hydrogen-bonded protons must have significantly smaller hyperfine coupling and a longer O . . . H distance.

Model of the SQ Environment

A protein-bound SQ can be stabilized as a neutral radical ($QH^\bullet$) or an anionic radical ($Q^{\bar{\bullet}}$), or in an intermediate state with partial charge remaining on the SQ. The location of the hydrogen atom along the H-bond relative to the quinone carbonyl determines the net charge on the SQ. As with any catalytic intermediate stabilized by an enzyme, the charge distribution of the bound SQ is clearly of mechanistic importance.

The transition from anionic to neutral form leads to changes in hyperfine couplings. These changes result from partial protonation of one of the carbonyl oxygens, leading to a shift of spin density and charge within the quinone ring. Protonation of carbonyl oxygen will stabilize more negative charge on the oxygen atom, which results in a shift of the spin density within the SQ. When O-1 is protonated, the increase in spin density is expected at carbons C1, C3, C5, and on O-4. On the other hand, O-4 protonation results in an increase in the spin density on atoms C2, C4, C6, and O-1 (38). These shifts in spin density are reflected in the EPR and ESEEM spectra, which can, therefore, be interpreted in terms of structural changes.

Wild Type Cytochrome bo_3—There are two strongly coupled exchangeable protons around the SQ in cytochrome bo_3. One of the protons (H2,$|T| = 6.3$ MHz) requires a very short O . . . H bond length, strongly indicating that the SQ species is a neutral radical. The 2-fold increase of the unpaired spin density at C5, with the attached methyl group, indicates protonation of the O-1 oxygen. The excess of negative charge on O-1 is postulated to result from a very strong, virtually covalent, H-bond with Asp-75, which facilitates the formation of a second hydrogen bond. The second proton is H3 ($|T| = 4.2$ MHz) observed in the ESEEM spectra. We favor the model that this proton is involved in H-bond between O-1 and a nitrogen donor from Arg-71 although the ESEEM data do not distinguish the assignment of the H-bonded nitrogen to the NH_2 or NH group of Arg-71 or to the Gln-101 side chain (Fig. 1). The two protons, H2 and H3, stabilize the strong asymmetry in the distribution of the unpaired spin density (and charge), which is observed.

It is noted that the asymmetrical H-bonding pattern exhibited by the SQ stabilized by cytochrome bo_3 is the opposite of that found for the SQ in the Q_A site of the bacterial reaction center (38). In the Q_A site, the O-4 carbonyl oxygen is

H-bonded to a histidine, His-M219, which results in shifting the negative charge toward O-4. It would, for instance, lead to the decrease of the spin density at the carbon with attached methyl group. The isotropic coupling of the methyl protons is ~5 MHz in the SQ at the Q_A site, *i.e.* smaller than that of an anion radical in solution, and consistent with the stronger protonation of the O-4 oxygen than the O-1 oxygen.

D75E Mutant—As with the wild type oxidase, there are two strongly coupled H-bonds to the SQ in the D75E mutant (supplementary materials Fig. S7). It is postulated that the SQ is still H-bonded to Asp-75 and Arg-71. The D75E replacement, however, weakens the H-bond with covalent character, and strengthens the H-bond with Arg-71. These two H-bonds still result in the significant asymmetric distribution of the unpaired spin density.

D75H Mutant—The SQ in D75H mutant has only one strong H-bond, which is postulated to be with the nitrogen of His-75. The assignment of His-75 as a H-bond donor in the D75H mutant is supported by the comparison with the Q_A site. The value of the anisotropic coupling $T = 4.6$ MHz indicates the formation of the H-bond with an O . . . H bond length of ~1.5 Å, which produces a substantial asymmetric distribution of the spin density in the SQ. This H-bond is to the O-1 carbonyl, as shown by the 8 MHz coupling of the methyl protons. There is not a strong H-bond with Arg-71 in the D75H mutant, further supporting the assignment of a strong H-bond between the O-1 carbonyl and His-75.

In all three samples, the HYSCORE spectra show the presence of weakly coupled exchangeable protons, H4, which are definitively not involved in H-bonding to the carbonyl oxygens. Currently, one can only speculate about the structural possibilities for these protons and their influence on the SQ stabilization.

Mechanistic Implications

The D75H mutant does not significantly influence the electrochemical properties of the stabilized SQ at the Q_H site (2). However, clearly the electron density within the quinone ring is markedly changed, along with the pattern of hydrogen bonding. It is these consequences of the mutation, which are doubtlessly related to the near complete loss of catalytic function. There is a 20% decrease in the asymmetry of the spin density distribution in the SQ state, as determined by the value of the hyperfine coupling to the methyl protons. This could, conceivably, influence the rate of electron transfer into or out of the SQ. Similarly, the change in hydrogen bonding could easily alter the coupled proton transfer, which must accompany the redox changes of the quinone at the Q_H site.

During the catalytic cycle, the quinone bound at the Q_H site must undergo oxidation and reduction, with the concomitant changes in protonation. With an anionic SQ as an intermediate, the conversion between the fully reduced quinone and the 1-electron oxidized SQ species is coupled to the loss of both protons from the dihydroubiquinol.

$$QH_2 \leftrightarrows Q^{\cdot -} + 1e^{-1} + 2H^{+} \leftrightarrows Q + 1e^{-1} \qquad \text{(Eq. 4)}$$

It is reasonable that altering the hydrogen bonding of any of the redox states of the quinone could have a strong influence on the rate of protonation or deprotonation of the quinone during catalysis, and this could become rate-limiting. For more conclusive mechanistic and theoretical considerations, full knowledge of the *single occupied molecular orbital* in the wild type protein and in the D75H mutant would be very desirable, as would experimental data on which step or steps in the catalytic cycle is blocked by the D75H mutation.

REFERENCES

1. Tsubaki, M., Hori, H., and Mogi, T. (2000) *J. Inorg. Biochem.* **82,** 19–25
2. Hellwig, P., Yano, T., Ohnishi, T., and Gennis, R. B. (2002) *Biochemistry* **41,** 10675–10679
3. Hellwig, P., Barquera, B., and Gennis, R. B. (2001) *Biochemistry* **40,** 1077–1082
4. Hellwig, P., Mogi, T., Tomson, F. L., Gennis, R. B., Iwata, J., Miyoshi, H., and Mantele, W. (1999) *Biochemistry* **38,** 14683–14689
5. Grimaldi, S., MacMillan, F., Ostermann, T., Ludwig, B., Michel, H., and Prisner, T. (2001) *Biochemistry* **40,** 1037–1043
6. Grimaldi, S., Ostermann, T., Weiden, N., Mogi, T., Miyoshi, H., Ludwig, B., Michel, H., Prisner, T., and MacMillan, F. (2003) *Biochemistry* **42,** 5632–5639
7. Puustinen, A., Verkhovsky, M. I., Morgan, J. E., Belevich, N. P., and Wikström, M. (1996) *Proc. Natl. Acad. Sci. U. S. A.* **93,** 1545–1548
8. Mogi, T., Sato-Watanabe, M., Miyoshi, H., and Orii, Y. (1999) *FEBS Lett.* **457,** 223–226
9. Musser, S. M., Stowell, M. H. B., Lee, H. K., Rumbley, J. N., and Chan, S. I. (1997) *Biochemistry* **36,** 894–902
10. Schultz, B. E., Edmondson, D. E., and Chan, S. I. (1998) *Biochemistry* **37,** 4160–4168
11. Kobayashi, K., Tagawa, S., and Mogi, T. (2000) *Biochemistry* **39,** 15620–15625
12. Wiertz, F. G. M., Richter, O.-M. H., Cherepanov, A. V., MacMillan, F., Ludwig, B., and de Vries, S. (2004) *FEBS Lett.* **575,** 127–130
13. Abramson, J., Riistama, S., Larsson, G., Jasaitis, A., Svensson-Ek, M., Laakkonen, L., Puustinen, A., Iwata, S., and Wikström, M. (2000) *Nat. Struct. Biol.* **7,** 910–917
14. Yap, L. L., Samoilova, R. I., Gennis, R. B., and Dikanov, S. A. (2006) *J. Biol. Chem.* **281,** 16879–16887
15. Veselov, A. V., Osborne, J. P., Gennis, R. B., and Scholes, C. P. (2000) *Biochemistry* **39,** 3169–3175
16. Hastings, S. F., Heathcote, P., Ingledew, W. J., and Rigby, S. E. J. (2000) *Eur. J. Biochem.* **267,** 5638–5645
17. Rumbley, J. N., Nickels, E. F., and Gennis, R. B. (1997) *Biochim. Biophys. Acta* **1340,** 131–142
18. Höfer, P., Grupp, A., Nebenführ, H., and Mehring, M. M. (1986) *Chem. Phys. Lett.* **132,** 279–284
19. Schweiger, A., and Jeschke, G. (2001) *Principles of Pulse Electron Paramagnetic Resonance*, pp. 359–405, Oxford University Press, Oxford
20. Dikanov, S. A., and Bowman, M. K. (1995) *J. Magn. Reson. A* **116,** 125–128
21. Dikanov, S. A., Tsvetkov, Y. D., Bowman, M. K., and Astashkin, A. V. (1982) *Chem. Phys. Lett.* **90,** 149–153
22. Flanagan, H., and Singel, D. J. (1987) *J. Chem. Phys.* **87,** 5606–5616
23. Reijerse, E. J., and Dikanov, S. A. (1991) *J. Chem. Phys.* **95,** 836–845
24. Edmonds, D. T., and Summers, C. P. (1973) *J. Magn. Reson.* **12,** 134–142
25. Hunt, M. J., Mackay, A. L., and Edmonds, D. T. (1975) *Chem. Phys. Lett.* **34,** 473–475
26. Hunt, M. J., and Mackay, A. L. (1976) *J. Magn. Reson.* **22,** 295–301
27. McDowell, C. A., Naito, A., Sastry, D. L., and Takegoshi, K. (1986) *J. Magn. Reson.* **69,** 283–292
28. Ashby, C. I. H., Cheng, C. P., and Brown, T. L. (1978) *J. Am. Chem. Soc.* **100,** 6057–6063
29. Mims, W. B., and Peisach, J. (1978) *J. Chem. Phys.* **69,** 4921–4930
30. Jiang, F., McCracken, J., and Peisach, J. (1990) *J. Am. Chem. Soc.* **112,** 9035–9044

31. MacMillan, F., Lendzian, F., and Lubitz, W. (1995) *Magn. Reson. Chem.* **33,** 581–593
32. Joela, H., Kasa, S., Lehtovuori, P., and Bech, M. (1997) *Acta Chem. Scand.* **51,** 233–241
33. Samoilova, R. I., van Liemt, W., Steggerda, W. F., Lugtenburg, J., Hoff, A. J., Spoyalov, A. P., Tyryshkin, A. M., Gritzan, N. P., and Tsvetkov, Y. D. (1994) *J. Chem. Soc. Perkin Trans. I* **2,** 609–614
34. McConnell, H. M. (1956) *J. Chem. Phys.* **24,** 764–768
35. O'Malley, P. J., and Babcock, G. T. (1986) *J. Am. Chem. Soc.* **108,** 3995–4001
36. Flores, M., Isaacson, R. A., Calvo, R., Feher, G., and Lubitz, W. (2003) *Chem. Phys.* **294,** 401–413
37. Sinnecker, S., Reijerse, E., Neese, F., and Lubitz, W. (2004) *J. Am. Chem. Soc.* **126,** 3280–3290
38. Lubitz, W., and Feher, G. (1999) *Appl. Magn. Reson.* **17,** 1–49
39. Deligiannakis, Y., Hanley, J., and Rutherford, A. W. (1999) *J. Am. Chem. Soc.* **121,** 7653–7664
40. Astashkin, A. V., Kawamori, A., Kodera, Y., Kuroiwa, S., and Akabori, K. (1995) *J. Chem. Phys.* **102,** 5583–5588
41. Lendzian, F., Rautter, J., Käß, H., Gardiner, A., and Lubitz, W. (1996) *Ber. Bunsenges. Phys. Chem.* **100,** 2036–2040
42. Spoyalov, A. P., Hulsebosch, R. J., Shochat, S., Gast, P., and Hoff, A. J. (1996) *Chem. Phys. Lett.* **263,** 715–720